

Supporting Information

Temperature dependent amplified spontaneous emission of vacuum annealed perovskite films

**Liang Qin,^a Longfeng Lv,^a Chunhai Li,^a Lijie Zhu,^a Qihong Cui,^a Yufeng Hu,^a Zhidong
Lou,^a Feng Teng^a and Yanbing Hou^{*a}**

Key Laboratory of Luminescence and Optical Information, Ministry of Education, Beijing
JiaoTong University, Beijing 100044, China. E-mail: ybhou@bjtu.edu.cn

Contents

- Figure S1. The SEM images of the perovskite films vacuumed at different times.
- Figure S2. The XRD patterns of the perovskite films under different vacuum-times.
- Figure S3. The ASE threshold performance of the perovskite films under different vacuum-times.
- Figure S4. Schematic of the optical measurement setup.
- Figure S5. The ASE net gain and loss performance of each samples.
- Table S1. ASE characteristics of each vacuum treated perovskite thin films.
- Figure S6. Temperature dependent PL spectra of the rough film and the optimized film.
- Figure S7. The analyzation of the temperature dependent XRD patterns.
- Figure S8. The exciton binding energy estimated from temperature dependent absorption spectra.
- Figure S9. The exciton binding energy estimated from temperature dependent PL spectra

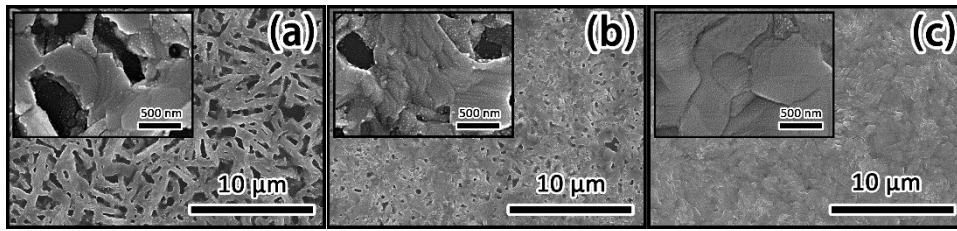


Fig. S1. The SEM images of the perovskite films vacuumed at 0 min (a), 5 mins (b) and more than 10 mins (c) before annealing. By increasing the vacuum-time, the morphology of the perovskite film is promoted. A dense, smooth and pore-free film was obtained by vacuuming more than 10 mins.

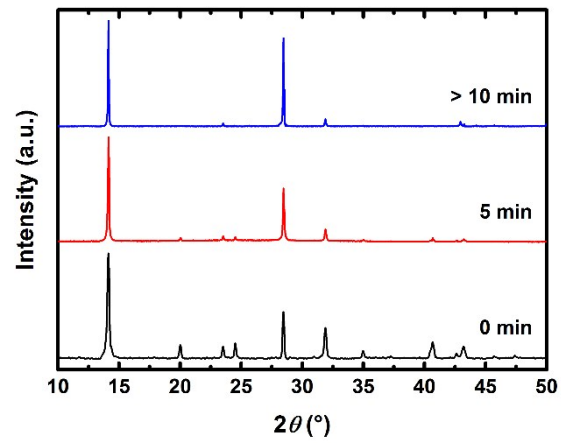


Fig. S2. The XRD patterns of the perovskite films vacuumed at 0 min, 5 mins and more than 10 mins before annealing. By increasing the vacuum-time, the perovskite film exhibit higher crystallinity and more ultra-uniform surface.

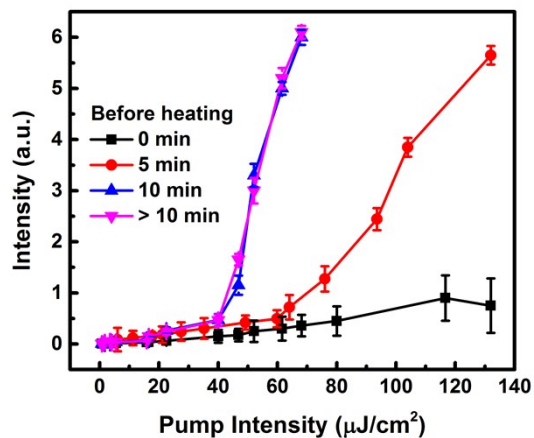


Fig. S3. The pump intensity effect on the output intensity of the perovskite films vacuumed at 0 min, 5 mins and more than 10 mins before annealing. The ASE performance measured from the MAPbI_3 perovskite films in Fig. S1 shows that the optimized film (vacuumed more than 10 mins) exhibits a well ASE performance with the threshold of $\sim 40 \mu\text{J}/\text{cm}^2$.

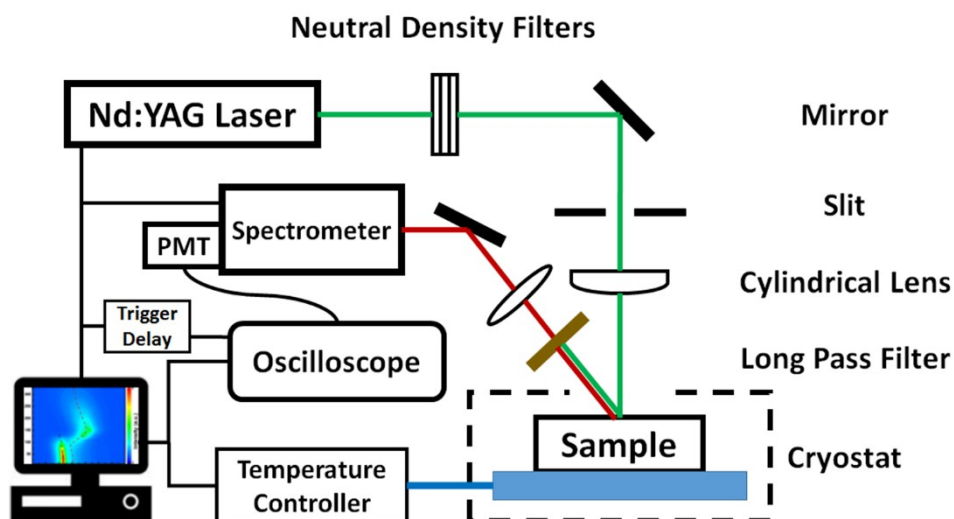


Figure S4. Schematic of the optical measurement setup. All samples were optically pumped at 500 nm by an optical parametric oscillator that delivered 5-ns pulses at a repetition rate of 10 Hz, itself pumped by a Q-switched, neodymium ion-doped, yttrium aluminum garnet (Nd³⁺:YAG) laser. The intensity of the laser was adjusted with neutral density filters of different transmittance. A $0.5 \times 3 \text{ mm}^2$ laser excitation strip was focused on the MAPbI₃ film with a cylindrical lens and an adjustable slit. The samples were held in a temperature-controlled cryostat. The emitting light from the sample of MAPbI₃ films was focused into a grating spectrometer through a long pass filter. The signal was amplified by a photomultiplier and coupled into an oscilloscope. All the measurement and instruments were controlled by a self-designed software.

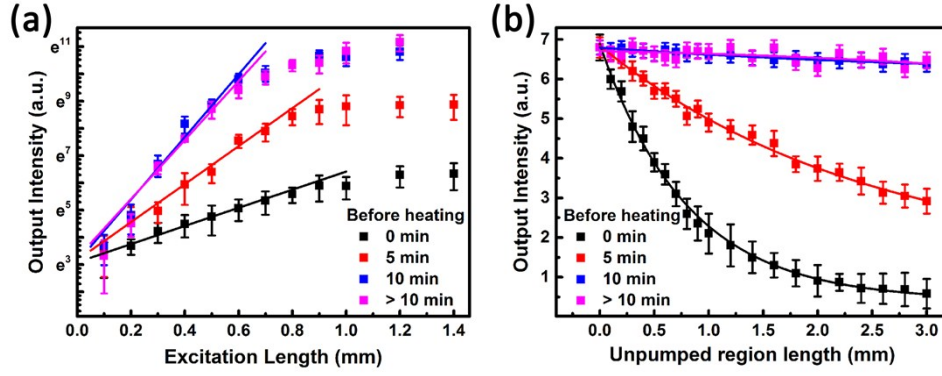


Figure S5. The ASE net gain fitted by the dependence of output intensity on excitation length (a), and the loss coefficient fitted by the output intensity on un-pumped region (b) of the perovskite films prepared by the vacuum treatment under 0 min, 5 min, 10 min and more before annealing.

The net gain was calculated by the usual variable-strip-length method, at room temperature in the air, in which the relationship between ASE emission $I(\lambda)$ and the length of excitation strip can be given by the following equation.¹

$$I(\lambda) = \frac{A(\lambda)I_p}{g(\lambda)}(e^{g(\lambda)L} - 1)$$

where $A(\lambda)$ is a constant related to the cross section for spontaneous emission, I_p is the pump intensity, $g(\lambda)$ is the net gain coefficient, and L is the length of the pumped strip. Figure 1(a) shows the excitation length dependences of ASE output intensity of samples vacuumed at different time before annealing. The solid line in Figure 1(a) is a linear fit of the initial part of the half-logarithmic plot of the experimental data which is shown in Table 1. From the fitness results, the net gain is $29.18 \pm 0.34 \text{ cm}^{-1}$ of the sample without vacuum treatment. With the vacuum treatment time more than 10 min before annealing, the ASE net gain is significantly increased to $138.75 \pm 0.91 \text{ cm}^{-1}$, which is clear that vacuum treatment increasing the net gain.

The loss coefficient of the thin film waveguide was measured using a regular method in which the pumped length was kept constant ($L = 3 \text{ mm}$) and the pumped region was moved away from the edge of the waveguide. Because the excitation of the pump strip remains constant, the detected ASE output from the edge of the sample decreases as the un-pumped region from the end of the pump region to the edge increases in length with the following equation.¹

$$I = I_0 e^{-\alpha x}$$

where α is the waveguide loss coefficient and x is the length of the un-pumped region from the end of the pump region to the edge of the sample.

Table S1. ASE characteristics of each vacuum treated perovskite thin films

Vacuum treatment (min)	Threshold ($\mu\text{J}/\text{cm}^2$)	Gain (cm^{-1})	Loss (cm^{-1})
0	95.4 ± 10.65	29.18 ± 0.34	12.49 ± 0.68
5	61.70 ± 2.65	68.73 ± 0.38	4.83 ± 0.64
10	40.42 ± 1.48	137.18 ± 1.10	2.53 ± 0.44
>10	42.30 ± 1.45	138.75 ± 0.91	2.63 ± 0.62

All the parameters are the average of 10 times.

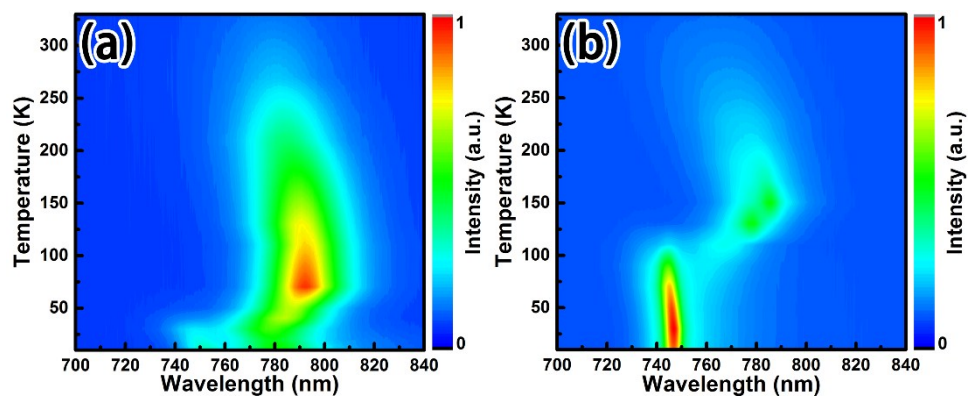


Fig. S6. Temperature dependent PL spectra of the rough film (Fig. 1(b)) and the optimized film (Fig. 1 (c)) respectively. It indicates that a completely transition from tetragonal phase to orthorhombic phase occurs in the optimized film and strong PL intensity during the phase transition.

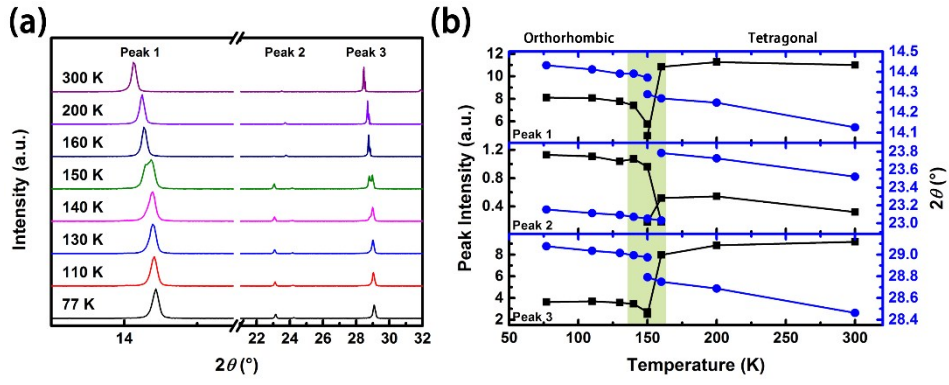


Fig. S7. (a) Typical peaks of XRD patterns, at $\sim 14.37^\circ$, $\sim 23.07^\circ$ and $\sim 28.99^\circ$, at different temperatures from 77 K to 300 K. (b) The position and the intensity of these three peaks as a function of temperatures.

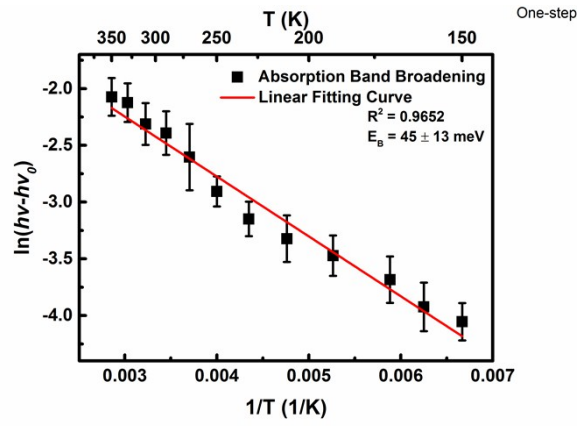


Fig. S8. The estimation of the exciton binding energy via temperature dependent absorption spectra. The binding energy of $45 \pm 13 \text{ meV}$ is estimated from the temperature-independent broadening equations.²

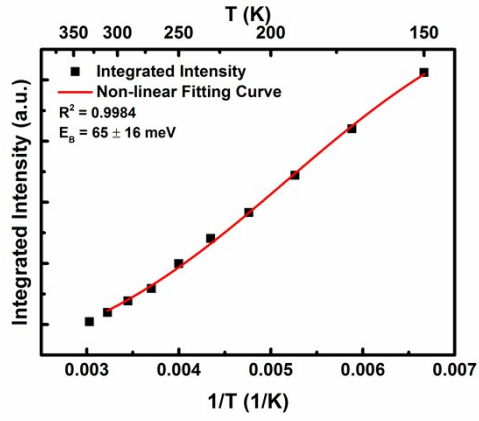


Fig. S9. The estimation of the exciton binding energy via peak intensity of temperature dependent PL spectra. The binding energy of 65 ± 16 meV is estimated from the temperature-dependent free excitons emission intensity equations.³

References:

1. M. D. McGehee, R. Gupta, S. Veenstra, E. K. Miller, M. A. Diaz-Garcia and A. J. Heeger, *Phys. Rev. B*, 1998, **58**, 7035.
2. V. D'Innocenzo, G. Grancini, M. J. Alcocer, A. R. Kandada, S. D. Stranks, M. M. Lee, G. Lanzani, H. J. Snaith and A. Petrozza, *Nat. Commun.*, 2014, **5**, 3586.
3. K. Wu, A. Bera, C. Ma, Y. Du, Y. Yang, L. Li and T. Wu, *Phys. Chem. Chem. Phys.*, 2014, **16**, 22476-22481.